LIMNOLOGY
and
OCEANOGRAPHY: METHODS

ASLO

Limnol. Oceanogr.: Methods 13, 2015, 15–29

doi: 10.1002/lom3.10003

A comparison of methods for the measurement of CO_2 and CH_4 emissions from surface water reservoirs: Results from an international workshop held at Three Gorges Dam, June 2012

Yan Zhao,[1] Bradford Sherman,*[2] Phillip Ford,[2] Maud Demarty,[3] Tonya DelSontro,[4,5] Atle Harby,[6] Alain Tremblay,[7] Ida Beathe Øverjordet,[8] Xinfeng Zhao,[1] Bjørn Henrik Hansen,[8] Bingfang Wu[1]

[1]Key Laboratory of Digital Earth Sciences, Institute of Remote Sensing and Digital Earth, Chinese Academy of Sciences, Beijing, China
[2]CSIRO Land and Water, Catchment biogeochemistry and aquatic ecology, Black Mountain, Australian Capital Territory, Australia
[3]Environnement Illimité Inc., Montréal, Québec, Canada
[4]Eawag: Swiss Federal Institute of Aquatic Science and Technology, Kastanienbaum, Switzerland
[5]Institute of Biogeochemistry and Pollutant Dynamics, ETH Zürich, Zürich, Switzerland
[6]SINTEF Energy Research, Energy Systems, Trondheim, Norway
[7]Hydro-Québec Production, Montréal, Québec, Canada
[8]SINTEF Materials and Chemistry, Environmental Technology, Trondheim, Norway

Abstract

Fluxes of carbon dioxide (CO_2) and methane (CH_4) from hydroelectric and water supply reservoirs are receiving increasing attention around the world with a number of research groups having undertaken measurements of these emissions across a range of lakes and reservoirs located in different climates and landscapes. The use of floating chambers (aka flux chambers) is the most common technique for direct measurement of these fluxes. However, the relative performance of different measurement systems, especially different chamber designs, is not well documented. We report the results of an international workshop held in June 2012 at Three Gorges Dam, China, to compare measurements performed by four groups with extensive chamber monitoring experience: the Chinese Academy of Science (China), CSIRO (Australia), SINTEF (Norway), Hydro-Québec/Environnement Illimité (Canada). A fifth group, Eawag (Switzerland), performed hydroacoustic surveys to detect ebullition in the water column. We recommend CH_4 as a more suitable trace gas for comparing methodologies due to its relative stability in the surface layer of the water column, for example, it is not subject to significant diurnal changes due to photosynthesis and respiration. Measured fluxes agreed to within 20% between the four teams suggesting that the shape and dimensions of the floating chambers and the chamber gas flow rates (i.e., chamber residence time) did not have an appreciable systematic effect on the measured fluxes for the relatively low wind speeds prevalent at the reservoir. The CO_2 and CH_4 fluxes measured during the workshop agree well with previous measurements in Three Gorges Reservoir.

Over past decades, much research has revealed that inland waters, including rivers, lakes, and reservoirs are potential sources of atmospheric greenhouse gases (GHG) including CO_2, CH_4, and N_2O. GHG emissions from hydroelectric reservoirs have raised special concerns due to the alteration of carbon dynamics resulting from the introduction of dams (Rudd et al. 1993; Kelly et al. 1997; Fearnside 2002). Most research has been undertaken in reservoirs mainly located in tropical and boreal regions where results have confirmed that net emissions from reservoirs may contribute to global warming to varying degrees, although the physical and biogeochemical processes are not clear yet (Teodoru et al. 2011). Based on a limited data set, St Louis et al. (2000) first estimated that the total emissions from reservoirs were up to 70 Tg CH_4 yr^{-1} and 1000 Tg CO_2 yr^{-1}, which accounted for 7% of the anthropogenic emissions of these gases. Barros et al. (2011) recently estimated that hydroelectric reservoirs only emitted 176 Tg CO_2 yr^{-1} and 4 Tg CH_4 yr^{-1} based on emissions from 85 reservoirs distributed worldwide. It is believed that there are still large uncertainties in these quantifications of global emissions due to the high variability of gas emissions from different reservoirs and limited available data (Diem et al. 2012). The high variability in emission estimates highlights the need for accurate measurements of

*Correspondence: csiro.brad@me.com

GHG emissions from hydroelectric reservoirs and an understanding of how comparable different measurement methodologies are.

To understand GHG emissions from water bodies it is necessary to understand gas transfer across the water-atmosphere interface, a topic that has long been studied. Much of the early research conducted in the 1950s and 1960s was undertaken by chemical engineers to facilitate better process understanding (e.g., Danckwerts 1951; Downing and Truesdale 1955). Concern about the capacity of natural waters to assimilate effluents with a large oxygen demand motivated much research in the 1960s, for example, Dobbins (1964), and this work has found itself incorporated into several water quality models. The focus on rivers led to models that expressed gas transfer coefficients in terms of factors that could be related to the generation of turbulence, especially turbulence produced within the water column. Development of water quality models for standing waters such as lakes and reservoirs and interest in gas exchange between atmosphere and ocean required a focus on turbulent kinetic energy (TKE) input at the air-water interface and many laboratory and field studies of the wind speed and wave field dependence of gas transfer have been undertaken (e.g., Kanwisher 1963; Jähne et al. 1979; Peng et al. 1979; Merlivat and Memery 1983; O'Connor 1983).

Deacon (1977) and O'Connor (1983) proposed two of the most influential parameterizations of gas transfer used in water quality models of the 1970s and 1980s. These models consider transfer across a water surface using a "resistance-in-parallel" formula in which the computed gas transfer velocity varies from the "stagnant film" model for quiescent systems to Danckwerts's (1951) "film replacement" model at higher levels of turbulence. Danckwerts (1951) provides a thorough analytical treatment of gas absorption through a liquid interface and proposed that a surface renewal model may be more appropriate than a "stagnant film" (i.e., constant boundary layer thickness) model. In the surface renewal model, the flux of the gas is controlled by the rate of replacement of the surface layer as opposed the stagnant film model's assumption of a changing boundary layer thickness through which Fickian diffusion drives the flux. The important feature of these models is that they recognize that gas transfer depends on turbulence within the water column and that turbulence is produced by multiple mechanisms.

Münsterer and Jähne (1998) conducted elegant boundary layer visualization experiments in a wind-water tunnel and found the concentration profile in the boundary layer on the water side of the air-water interface was best represented using a surface renewal model with a Schmidt number exponent of 2/3.

The dominant paradigm has become the Thin Boundary Layer (TBL) model most commonly attributed to Liss and Slater (1974) although already referred to in essence by the earliest researchers such as Danckwerts (1951). The TBL model is the foundation of most large-scale estimates of aquatic GHG emissions. It can be thought of as a "stagnant film" model in which the thickness of the boundary layer decreases with increasing wind speed. The TBL computes the gas flux as the product of a gas transfer velocity and a gas concentration difference. The most common wind speed relations used to compute the gas transfer velocity for TBL calculations are those of Cole and Caraco (1998), Wanninkhof (1992), and MacIntyre et al. (2010). These parameterizations were derived from data collected from a range of natural systems where different processes likely dominated TKE input at the water surface, for example, Cole and Caraco (1998) focused on low wind speeds whereas Wanninkhof (1992) used ocean data with wind speeds mainly > 4.5 m s^{-1}. Significantly, application of models using either the TBL or surface renewal paradigms are only as good as the direct flux measurements used to calibrate them.

Relatively recently, the importance of penetrative convection as a source of TKE in low wind speed environments has been documented (MacIntyre et al. 2010). Schladow et al. (2002) demonstrated the influence of penetrative convection on oxygen transfer. Vachon et al. (2010) confirm the fundamental role of turbulence in the water column near the air-water interface governing the gas transfer velocity.

An important source of uncertainty in our knowledge of reservoir gas fluxes arises from the measurements we use to directly quantify them. The two most common direct flux measurement techniques are floating chambers (FCs) and eddy covariance systems. Of these two, the most frequently used technique is the FC method (Duchemin et al. 1995; St Louis et al. 2000; Podgrajsek et al. 2013). Flux estimation using the TBL method incorporates uncertainties inherent in the measurements of dissolved gas concentration and wind speed used to determine the gas transfer velocity (Cole et al. 2010).

The FC method involves measuring, over time, the change in chamber head space gas concentration. Originally, these measurements were undertaken using gas chromatography to analyze discrete samples taken from the chambers. During the 1990s, on-line gas analyzers provided near-continuous time series of CO_2 data but were often not sensitive enough to provide successful measurements of CH_4 fluxes (Tremblay et al. 2005). Trace gas analysis has recently undergone a revolution with the advent of high frequency and high precision instrumentation for the measurement of both CO_2 and CH_4. This has made feasible simultaneous rapid measurement of fluxes of both gases. The introduction of the new generation of gas analyzers such as cavity-ring-down spectrometers (CRDS) with sub-ppb resolution for CH_4 measurement, allow real-time measurements of CH_4 flux under low flux conditions as well as allowing detection of individual bubble events of CH_4 entering the chambers, a process not detected in the two point measurements (beginning and end) which characterized the earlier generation of chamber measurements.

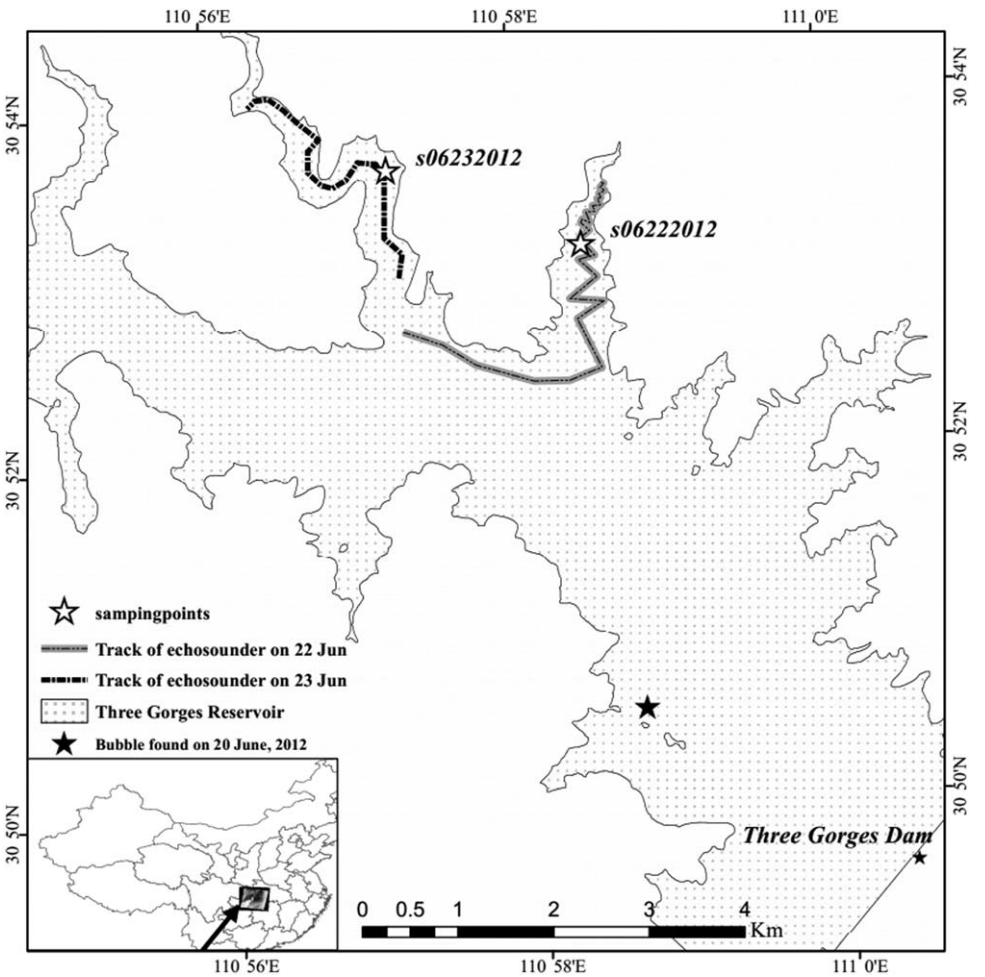

Fig. 1. Site map. Stars denote measurement vessel locations on 20 June 2012, 22 June 2012, and 23 June 2012. Lines show the echosounder tracks for the hydroacoustic bubble detection surveys.

Numerous flux chamber designs have been developed and applied, although the physical principals have sometimes been overtaken by convenience and practicality with designs ranging from upturned buckets to higher engineered chambers with floats tuned to the prevailing water conditions. The history of application of different methods under different conditions makes it challenging to discriminate between affects arising from environmental conditions, different analytical instruments, and different chamber designs. These differences can only be identified and resolved by intercomparison of techniques under the same conditions. Recent examples include the differences between techniques using eddy covariance, flux chambers, anchored funnels, and boundary layer models (Peltola et al. 2013; Podgrajsek et al. 2013; Peltola et al. 2014) and Gålfalk et al.'s (2013) comparison of flux chamber, acoustic doppler velocimetry (ADV), and infrared imaging techniques.

Here, we report on an intercomparison experiment to compare the performance of four FC measurement methodologies made under nominally the same conditions at the same location, and minimum separation. In addition, hydroacoustic surveys were undertaken to detect and quantify the presence and extent of rising bubble plumes.

Materials and Procedures

Site description

The experiment was carried out in Three Gorges Reservoir, at a region about six kilometers upstream from the Three Gorges Dam located between 30°50′N–30°54′N and 110°55′E–111°E) (Fig. 1). The climate of this region is dominated by the subtropical monsoon (June to September), and has a mean annual temperature of 18°C. In June (summer), the average daily temperature can reach up to 30°.

Measurements were taken at three different locations on 20 June 2012, 22 June 2012, and 23 June 2012. On 20 June, a test measurement was taken on the southern side of the reservoir in open water about 3.5 km upstream of the dam. On 22 June,

Table 1. Chamber configurations.

Group	Gas analyzer	Recircled air?	Height (m)	Skirt Depth (m)	Volume (L)	Area (m^2)	Tube length (m)	Tube dia (mm)	Qair ($L\ min^{-1}$)
CAS	Picarro G2301	No	0.55	0.050	38.9	0.07	4	4	0.2
CSIRO	Picarro G1301	Yes	0.166	0.140	33.6	0.203	4	6	5
EI	Picarro G1301	Yes	0.110	0.190	17.6	0.16	4	6	2.8
SINTEF	Picarro G2301	Yes	0.136*	0.050	25.8	0.189	5	6	5.5

*denotes an equivalent mean height (= Vol/Area) for the SINTEF chambers which have sloping sides; their volume was directly measured.

measurements were undertaken in the sheltered inlet of Hanjia Bay (site s06222012) and on 23 June in the inlet of Baisuixi further upstream from the dam (site s06232012).

Cross sections of the main channel in this region have a U-shape with a maximum depth of $\sim$ 170 m when at full storage level (FSL = 175 m a.s.l.). There are several small tributaries within the region, where the water is much shallower (from less than 30 m at their upstream ends to over 100 m where they meet the main basin). River flow in this region exhibits significant seasonal variability due to normal operation of the dam. Discharge from the dam varies seasonally from 5000 $m^3\ s^{-1}$ December to April to $>$ 35,000 $m^3\ s^{-1}$ following the June to September monsoon season. The discharge range produces mean water column velocities in the range of 0.05–0.5 m s^{-1} in the main basin while in the small tributaries the water is almost still.

A combination of relatively high water velocities and low solar insolation due to the tall, steep gorge walls serve to reduce stratification during most of the year relative to many other reservoirs. Previous observations have revealed that Three Gorges Reservoir is generally well mixed from top to bottom most of the year with dissolved oxygen (DO) concentrations in the range 7–9 mg L^{-1}. Only in April and May, after seasonal heating has commenced but before the large discharges caused by the summer monsoon arrive, are there substantial differences in water column temperature (up to 6°C) and DO (2–3 mg L^{-1}) in both the main basin and tributaries (Yu and Wang 2011; Zhao et al. 2013). Under warm season conditions, the reservoir is prone to algal blooms with Chlorophyll-a concentrations sometimes $\geq$ 200 μg/L.

Flux measurement experiment

The flux measurement experiment was carried out from 22 June 2012 to 23 June 2012. Two sampling sites were selected in the middle reach of two tributaries in the region. The main channel of the reservoir is busy with shipping traffic and it is not allowed to float on the channel for extended periods. Water depths of the two sites were 20 m (s22062012, Fig. 1) and 43 m (s23062012, Fig. 1), respectively. The boat used for the sampling was anchored after arrival at the sites.

Four teams, Chinese Academy of Science (CAS), Commonwealth Scientific and Industrial Research Organization (CSIRO), Hydro-Québec/Environnement Illimité (HQ/EI), and SINTEF performed flux chamber measurements from one boat while the Eawag team undertook hydroacoustic surveys using a second boat. The teams used a combination of different chamber designs and sampling methodologies described in greater detail below (Table 1). The relative locations of the flux chamber systems are shown to scale in Fig. 2. Measurements did not commence until all visible disturbance caused by the boat had disappeared. There was little if any perceptible water motion around the boat during the experiment, that is, no visible wakes produced by the chambers.

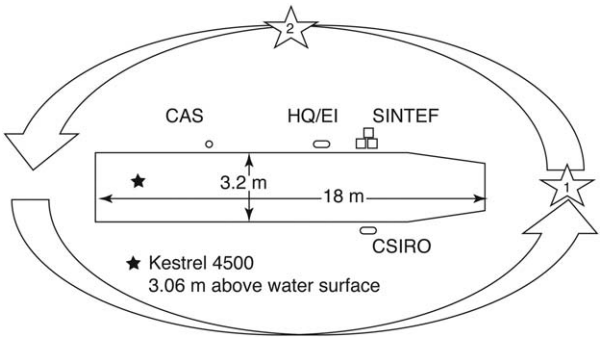

Fig. 2. Location of the four FCs relative to the boat. Stars 1 and 2 denote location of bubble plumes identified using hydroacoustics (ca. 10 m from boat). Large arrows denote path of hydroacoustic survey around the main boat. Filled star denotes location of Kestrel 4500 deployed on the roof of the boat to measure wind speed and direction at a height of 3.06 m above the water surface.

The four groups performed continuous consecutive deployments for the duration of each day. Due to the different methodologies used, the deployments were not always concurrent. Each team would place their chamber on the water surface to start sampling, and after a nominal 15 min interval, the chamber was pulled out from the water and opened to the atmosphere. After the air in the chamber was fully mixed with the atmosphere, the chamber was redeployed to start another round of measurements.

FC system designs

Table 1 lists the major characteristics of the four FC measurement systems. All teams used CRDS manufactured by Picarro. The CSIRO and HQ/EI teams used the Picarro G1301 while SINTEF and CAS used the Picarro G2301. Prior to adoption of a CRDS, the HQ/EI team had for years used

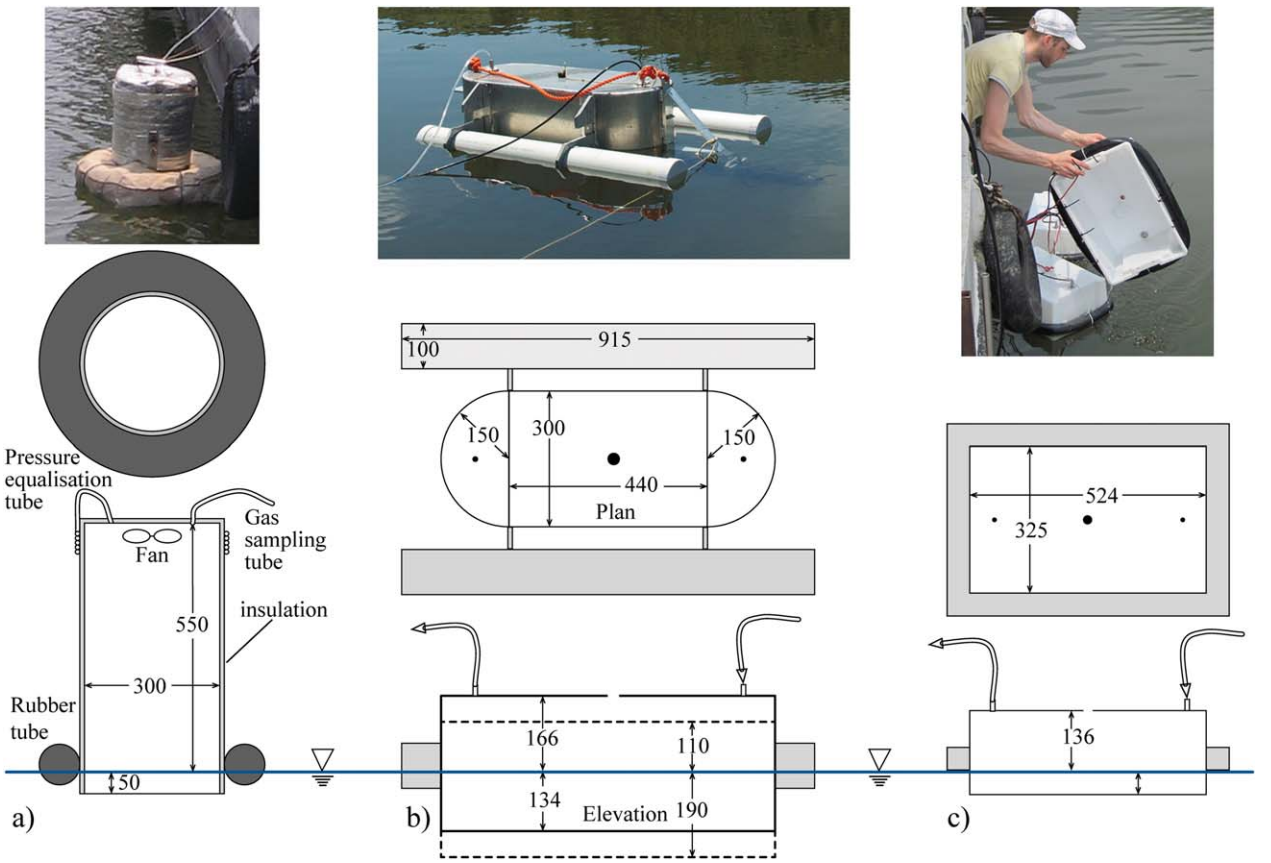

Fig. 3. FCs used by (a) CAS; (b) CSIRO (solid line) and HQEI (dashed line); and (c) SINTEF. Note that float dimensions in (b) are shown for the CSIRO chamber. Also shown in the photo in (b) is the Nortek ADV deployed beneath the CSIRO chamber.

Non-Dispersive Infra-Red (NDIR) and Fourier Transform Infrared gas analyzers, which required desiccation of the gas samples prior to analysis (Tremblay et al. 2005). None of the teams desiccated their samples during the experiment. The Picarro instrument outputs both "raw" and "dry" CH_4 concentration data by applying a correction based on the measured water vapor content. CSIRO used "raw" CH_4 data to compute fluxes whereas the other teams used the "dry" CH_4 concentration data. In practice, flux measurements are not much affected by the choice of CH_4 data unless there is a large change in water vapor content during the course of a chamber deployment, an occurrence which is very rare in our experience.

Three different chamber designs were used. CSIRO and HQ/EI used the same shaped (rectangle with round ends) aluminum chambers supported by polyvinyl chloride floats but with different head space heights, that is, the chamber edges (skirt depth) penetrated the water by different amounts (Table 1). SINTEF used three plastic rectangular chambers with slightly sloping side walls having an average head space height (Volume/Area) of 136 mm and a skirt depth of approximately 50 mm. The SINTEF chambers were supported using inflatable rubber tubes. The CAS chamber was cylindrical, 300 mm in diameter, constructed of steel and covered with a thin insulating layer with a head space height of 550 mm and a skirt depth of 50 mm and was supported using an inflatable rubber tube (Fig. 3).

The recirculation and sampling systems differed between teams and the combination of different head space volumes and gas flow rates produced a range of chamber residence times from 4.5 to 7 min for the recirculating systems to 194 min for the CAS once-through system (Fig. 4). The CAS system used a fan to ensure well-mixed conditions within the chamber whereas the other three teams rely on the recirculation gas flow to mix the headspace gas. The CSIRO, HQ/EI, and SINTEF systems consisted of loops of 1/4 in. tubing roughly 8–10 m in total length through which the chamber headspace gas was recirculated using diaphragm pumps (KNF). A second loop of tubing was connected between the gas analyzer and the recirculation loop allowing the gas analyzers built-in pump to sample the headspace gas and return it to the recirculation loop. SINTEF's system consisted of three replicate chambers, each with their own recirculation loop. The three loops were connected to a valve

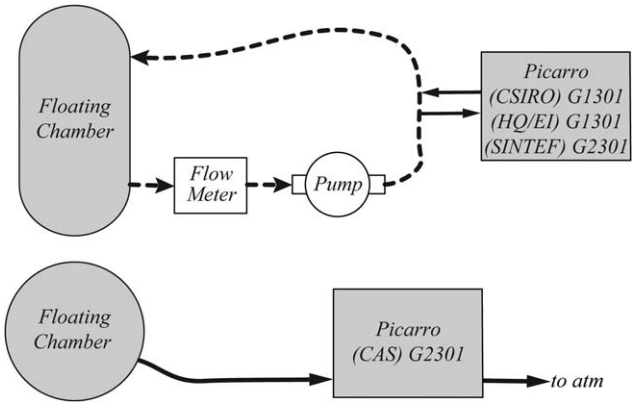

Fig. 4. Schematic diagram of gas flow through the different FC systems. Dashed line denotes the recirculation loop, and solid lines denote the gas sampling flow. Note that the CAS system discharged gas to the atmosphere following measurement. Recirculation (dashed lines) gas flow rates varied from 2.8–5.5 L min^{-1} whereas the gas sampling flow was driven by the gas analyzers sampling pump at a nominal rate of 200 mL min^{-1}.

electronically controlled by the gas analyzer allowing the gas analyzer loop to connect to any of the three chambers as required.

The CAS sampling system was quite different. The chamber contains a 12V fan to facilitate mixing of the headspace gas and uses the gas analyzer pump to sample the gas. The sampled gas is not recycled after the analysis but evacuated to the atmosphere (Fig. 4). A length of tubing wrapped around the chamber provided pressure equalization with the atmosphere (Fig. 3) in effect making this system a "once-through" system with admission of air through the pressure equalization tubing.

Hydroacoustic survey

Surveys of ebullition in the sampled tributaries (Fig. 1) were conducted both prior to and during the chamber measurements using a vertically downward oriented Simrad split-beam echosounder (EK60, 7° beam angle) with a 120 kHz transducer operating at a ping rate of five per second and a lower threshold of −120 dB. The echosounder was mounted about 30 cm below the water surface and calibrated with a 23 mm diameter standard copper target (DelSontro et al. 2010). The boat with the echosounder traveled at a low velocity along zigzag transects from the upstream end of each tributary to their confluences with the main channel. A small inverted funnel with an opening of ~ 0.1 m^2 was used to capture bubbles for determination of their gas composition to allow calculation of gas mass fluxes from the hydroacoustic volumetric flux data.

Meteorological and water column measurements

Local meteorological conditions (wind speed and direction, air temperature, relative humidity, barometric pressure) were measured with a portable digital weather station (Kestrel 4500) mounted on a tripod located on the roof of the boat in a location free of obstructions to the wind at a height 3 m above the water surface. Water temperature, DO, and pH at different water depths were recorded with a multi-parameter water quality instrument (YSI 6600). Water column CH_4 and CO_2 partial pressures were measured using a LiquiCel membrane exchanger coupled to a NDIR analyzer for CO_2 (PP System EGM400) and a tunable dye laser for CH_4 (Franatech).

On-site calibration

All gas analyzers were calibrated concurrently in the field on 23 June 2012. A series of 10 precision gas mixtures were produced by mixing zero air and a reference gas with nominal concentrations of 300 ppmv CH_4 and 10,000 ppmv CO_2 using Bronkhorst mass flow controllers with capacities of 150 and 6000 mL min^{-1}. The mass flow controllers have specified accuracies of ± 0.5% of the reading ± 0.1% of full scale. The gas mixtures were delivered to the four gas analyzers using lengths of 1/4 in. tubing.

The CSIRO G1301 was used as the reference gas analyzer for comparison with the other teams' gas analyzers. The CSIRO analyzer is routinely calibrated against a series of precision dilutions using reference gases at the CSIRO laboratory in Canberra. The linearity of the calibration was within 0.4% of the manufacturer's specification shortly before the Three Gorges Dam field experiment. In addition, comparison between the CSIRO G1301s output and independent measurement of CSIRO FluxNet Wilson's Promintory reference gas (pCH_4 = 1757.73 ± 2 ppb) was within 4 ppb of the reference gas.

During the field calibration at Three Gorges Dam, the zero air was determined to have concentrations of 0.653 ppmv CO_2 and 2.7386 ppmv CH_4. Depending on the process used to produce the zero gas, there may be CH_4 present even if no CO_2 is present due to the lower condensation point for CH_4. Furthermore, the reference gas concentrations were determined retrospectively to be 197.5 ppmv CH_4 and 9700 ppmv CO_2 based on the dilution series results and these values are specified as the nominal reference concentrations for the calibration. The concentrations of the 10 gas mixtures ranged from 0.65 to 1078.36 ppmv CO_2 and from 2.74 to 23.48 ppmv CH_4. Each mixture was stable to within (1 s.d.) 0.6 ppmv (CO_2) and 0.007 ppmv (CH_4) (Table 2).

Environmental conditions during the experiment

During the intercomparison experiment, the water level was 145.75 m above sea level and the discharge was 12,800 m^3 s^{-1}. Weather conditions during the experiment were hot and humid with the air temperature ranging from 29°C to 44°C and relative humidity from 39% to 42%. Skies were largely clear, but with considerable haze possibly the result of agricultural burning elsewhere in the region. Barometric pressure was quite stable at 1052–1057 mb.

Table 2. Calibration gas flow rates (mL min^{-1}), nominal reference concentrations (CH_{4n}, CO_{2n}), and concentrations measured by CSIRO on 23 June 2012. β is the mixing ratio between the reference gas, Qr, and zero air, Qz, flows. All concentrations are in ppmv. Standard deviations were measured by the CSIRO gas analyzer.

Qr (mL min^{-1})	Qz (mL min^{-1})	β	CO_{2n} (ppmv)	CO_2 (ppmv)	CO_2 s.d. (ppmv)	CH_{4n} (ppmv)	CH_4 (ppmv)	CH_4 s.d. (ppmv)
0	3700	0.000	0.65	0.65	0.15	2.74	2.74	0.0011
10	3700	0.003	26.80	24.72	0.19	3.26	3.26	0.0039
30	3700	0.008	78.66	76.56	0.58	4.31	4.30	0.0035
60	3700	0.016	155.43	155.34	0.20	5.85	5.85	0.0056
90	3700	0.024	230.98	231.71	0.17	7.36	7.38	0.0029
120	3700	0.031	305.34	307.39	0.12	8.86	8.90	0.0025
150	3700	0.039	378.55	381.76	0.10	10.33	10.38	0.0021
150	2700	0.053	511.14	514.64	0.15	12.99	13.05	0.0028
150	1200	0.111	1078.4	1076.7	0.16	24.38	24.34	0.0067
95	1200	0.073	712.19	709.67	0.30	17.03	16.98	0.0059

Results

Gas analyzer calibration

All four gas analyzers exhibited excellent linearity and accuracy in the hot (> 35°C) and humid conditions on the boat. Measured CO_2 and CH_4 concentrations were biased low by 0.2% compared to the specified reference gas concentrations. This could reflect a small bias in the performance of the mass flow controllers.

For the CH_4 calibration, residuals between the measured values and the linear regression best fits had a standard deviation of 0.0345 ppmv and a maximum deviation of 0.057 ppm. For the CO_2 calibration, residuals between the measured value and the linear regression best fits had a standard deviation of 2.13 ppmv and a maximum deviation of 3.39 ppm. All teams' measurements agreed with one another to better than 0.8%

CH_4 and CO_2 flux and wind speed measurements

During the experiment, the measured CO_2 fluxes ranged from −1814 to −422 mg m^{-2} d^{-1} for HQ/EI, −1354 to −542 mg m^{-2} d^{-1} for CSIRO, and −1648 to −680 mg m^{-2} d^{-1} for SINTEF. CO_2 data for the CAS system suffered from high noise levels; the cause of the noise could not be determined. The negative values mean the studied sites acted as a CO_2 sink during the experimental period. The CO_2 fluxes were similar to previous studies in the tributaries of Three Gorges Reservoir (Zhao et al. 2013).

CH_4 fluxes ranged from 0.65 to 14.35 mg m^{-2} d^{-1} for HQ/EI, 0.2 to 10.4 mg m^{-2} d^{-1} for CAS, 1.1 to 13.2 mg m^{-2} d^{-1} for CSIRO, and 1.2 to 12.2 mg m^{-2} d^{-1} for SINTEF indicating that the study region was a source of atmospheric CH_4 and were within the range obtained previously by Zhao et al. (2013) and Yang et al. (2012). The measured fluxes responded rapidly to changes in environmental conditions.

Figures 5, 6 show the wind speed and direction, pCH_4, pCO_2, CH_4 fluxes, and CO_2 fluxes measured by all the teams on 22 June 2012 and 23 June 2012. On 22 June, winds blew initially from the southeast (i.e., from the main basin of the reservoir) then became quite steady from the east at 1–2 m s^{-1} before dropping below the stall speed of the anemometer between 14:04 and 14:31. At 14:31, the wind speed picked up again to 1–2 m s^{-1} but with greater fluctuations in direction. At 16:38, there was an abrupt increase in speed from 1.3 to 5.9 m s^{-1} accompanied by a decrease in air temperature from 34.5°C to 30°C as the wind direction switched from easterly to northerly (from the gorge toward the main basin). On 23 June 2012, measurements were undertaken in a different tributary and winds blew fairly steadily from the north to northeast at 2.1 ± 0.5 m s^{-1}.

CH_4 fluxes exhibited a similar trend as wind speed on 22 June with local maximum (in time) fluxes lagging the peaks in wind speed by 30–50 min. The very large increase in flux corresponding to the increase in wind speed at 16:38 is described in greater detail below. On 23 June, CH_4 fluxes increased steadily as the wind speed increased, but were generally lower than on the previous day reflecting the much lower surface layer pCH_4 (section *pCO_2 and pCH_4*).

pCO_2 and pCH_4

Surface concentrations of dissolved CH_4 changed substantially during the 22 June 2012 deployment decreasing from 162 ppmv at 13:30 to 105 ppmv at 16:00 (Fig. 5). Given the unusual vertical profile of pCH_4 measured on 23 June 2013 with the highest concentration near the surface (Fig. 7) and the continuous stratification all the way to the water surface on both days, we believe this reflects the passage of water masses with differing concentrations through the measurement domain.

A single measurement for pCH_4 of 28.9 ppmv on 23 June 2012 was much different again from the preceding day's measurements presumably reflecting the fact that the measurements were made in a different tributary.

Surface layer pCO_2 also decreased markedly on 22 June but the decrease occurred earlier than the observed decrease

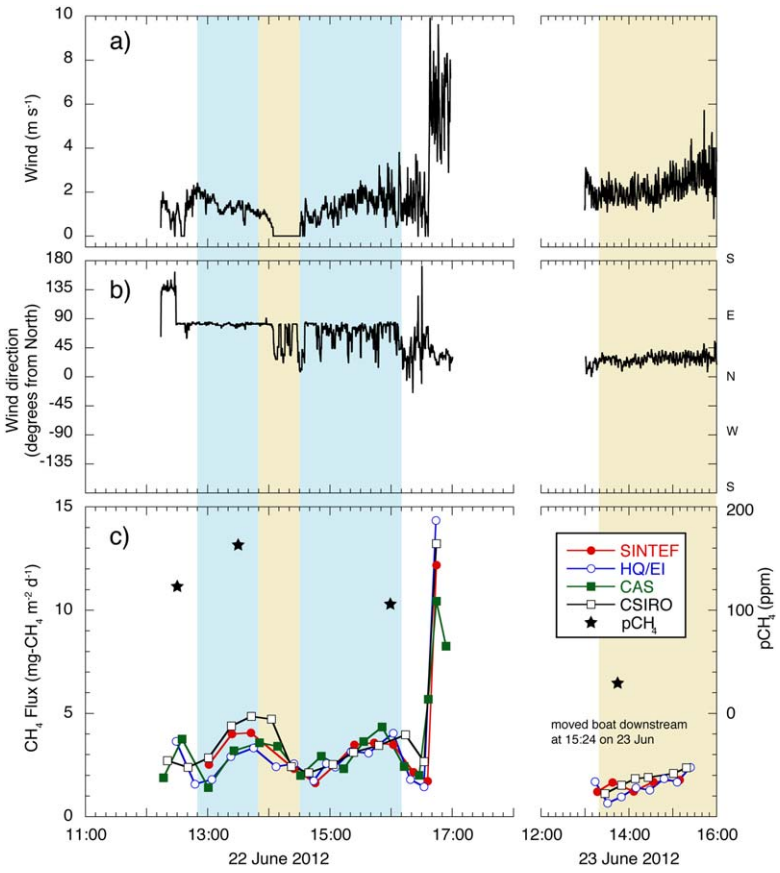

Fig. 5. (a) Wind speed and (b) direction at three m above the water surface, and (c) measured CH_4 fluxes (left axis) by the four teams using FCs and pCH_4 (right axis) measured by HQ/EI using the Franatech instrument at Three Gorges Dam on 22 June 2012 and 23 June 2012. Shaded bands denote periods used for statistical analysis in Figure 9.

in pCH_4 (Fig. 6). pCO_2 was higher on 23 June than on 22 June at the corresponding time of day consistent with our assertion of different water masses in the two different tributaries.

Flux response to step change in wind speed

On 22 June, at 16:38, both CO_2 and CH_4 fluxes were significantly increased when the wind speed changed from ~ 2 to ~ 6 m s^{-1}. Figure 8 shows raw gas analyzer CH_4 data for the four teams captured during the change in wind speed and Fig. 9 details the corresponding wind speed, wind direction, and ADV measurements of root-mean-square (RMS) velocity scale beneath the CSIRO chamber. Note that ADV velocities reflect the motion of the water relative to the chamber which was free to move within the constraints of the lengths of tubing used to recirculate the headspace gas. A prominent increase in RMS velocity scale follows the onset of the increase in wind speed with subsequent increases also apparently following changes in wind speed and/or direction.

Following the increase in wind speed, CH_4 fluxes increased by 606%, 890%, 84%, and 397% for SINTEF, HQ/EI, CAS, and CSIRO, respectively, whereas CO_2 fluxes (data not shown) changed by +20%, +40%, and −20% of their values before the wind change for SINTEF, HQ/EI, and CSIRO teams. Note that the calculated relative increase in flux is sensitive to the value of the small flux prior to the change in wind speed and this value could differ by up to 50% simply by shortening by 1–2 min the length of the data record used to compute the flux. The results here use the maximum length of record available.

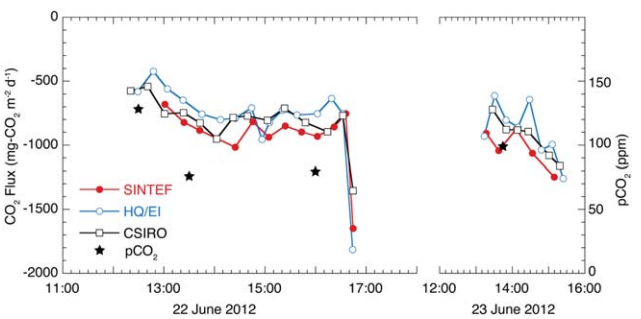

Fig. 6. CO_2 fluxes and surface layer pCO_2 measured at Three Gorges Dam on 22 June 2012 to 23 June 2012.

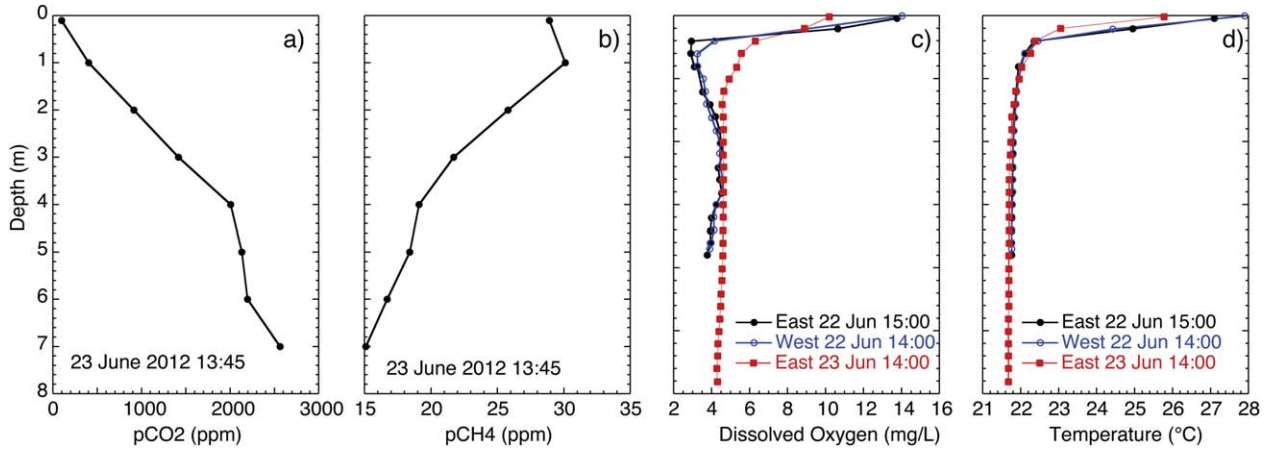

Fig. 7. Water column profiles of (a) pCO_2; (b) pCH_4; (c) DO; and (d) temperature. pCO_2 and pCH_4 were measured on 22 June using the Franatech instrument. Temperature and DO profiles were measured using an YSI v6600 sonde on both the east and west sides of the boat on 22 June 2012 and on the east side of the boat on 23 June 2012.

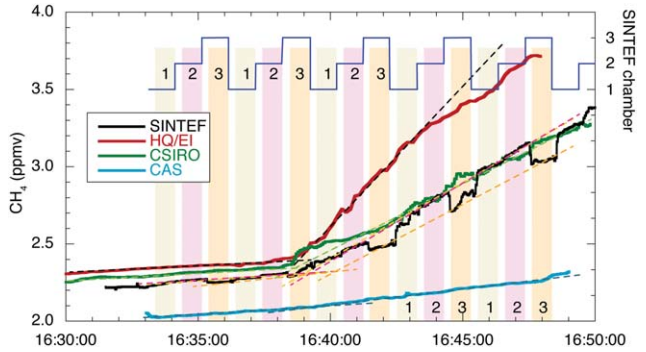

Fig. 8. Raw gas analyzer output for the four teams during the large step change in wind conditions on 22 June 2012. Shaded bars denote which of the three SINTEF chambers was being sampled. Dashed lines denote visual best fit to data before and after the wind change. Intersection of the before and after best-fit lines provides an indication of the time at which the change in flux occurred in response to the change in wind speed.

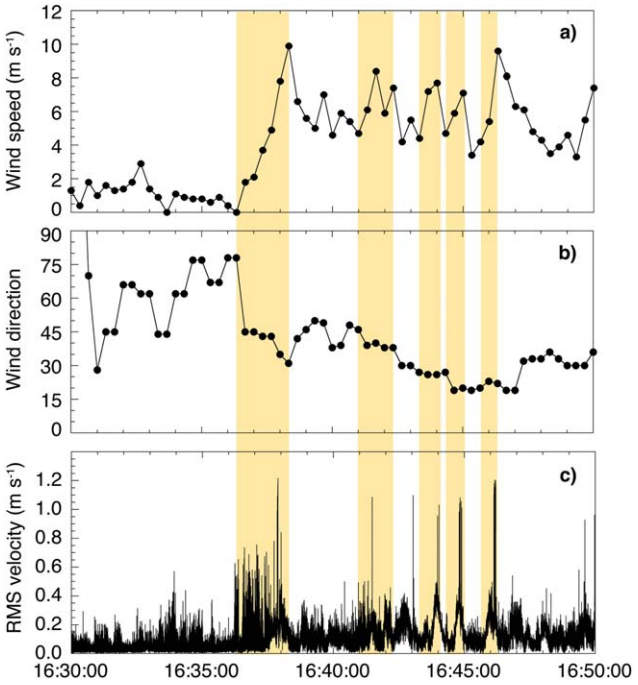

Fig. 9. (a) Wind speed, (b) direction, and (c) ADV-measured RMS velocity scale for water beneath the CSIRO chamber during the large step change in wind conditions on 22 June 2012. Shaded bars denote periods of accelerating wind speed.

HQ/EI measured > 100% greater increase in flux compared to CSIRO even though both teams used identical chambers but with different headspaces. The submerged edge of the HQ/EI chamber was 56 mm deeper than the CSIRO chamber. Also, the HQ/EI chamber was deployed from the side of the boat with greater exposure to the wind. The similar fluxes measured by both teams before the increase in wind speed suggests that surface layer pCH_4 was similar on both sides of the boat and that chamber-induced turbulence had negligible effect on the flux during the relatively calm period before 16:38. We believe that the difference between the HQ/EI and CSIRO measurements reflects mainly differences in the exposure of the chambers to the effect of the wind.

A conspicuous feature of the SINTEF data (Fig. 8) is the lower CH4 concentration reported by chamber 3 compared to the other two SINTEF chambers following the increase in wind speed. Because the slope, dCH_4/dt, is similar for all three chambers the computed fluxes are quite similar. The lower concentrations reported for chamber 3 may indicate a short delay in the onset of the higher flux into chamber 3—possibly reflecting very small scale (< 0.5 m) changes in water column turbulence and/or pCH_4.

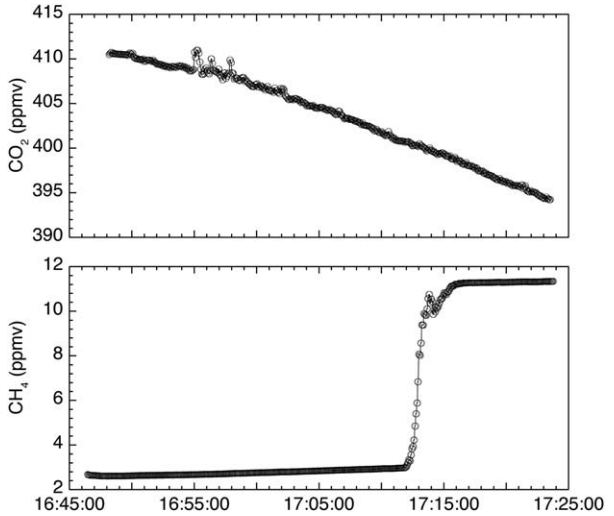

Fig. 10. CSIRO chamber CO_2 and CH_4 concentrations before and after entry of a bubble during a deployment at Three Gorges Dam on 20 June 2012. Linear regression is not a suitable method for calculating the CH_4 flux in these circumstances; it is better to simply use the end points of the time series.

Bubble detection results

CH_4 bubble events are easily observed in the real-time data displayed by the gas analyzers. When a bubble enters the chamber, the CH_4 concentration in the chamber will increase conspicuously and may also drop and rise again as the gas is mixed throughout the chamber (Fig. 10). Typically, little or no corresponding change in CO_2 concentration is detected. Taking this as an indicator of bubble events, during the two-day measurements, CAS captured four bubble events (out of 21 measurements in total), SINTEF captured one bubble event (out of 16 measurements × 3 replicate chambers), and CSIRO captured two events in 31 measurements. Measurements impacted by bubble events were excluded from further analysis.

The hydroacoustic surveys detected bubble activity emerging from the sediments both around the gas sampling sites and along the tributaries. However, the number of ebullition sites was relatively few, even at the upper reaches of the two tributaries with shallow water. The strongest bubble activity was observed at the downstream end of Hanjia Bay in deeper water (close to site s06222012). Few bubbles were observed to reach the water surface. Bubbles were very rare in the main channel. Due to the small size and low frequency of bubbles reaching the surface, it was not possible to capture enough bubbles to determine their volume and composition.

Discussion

Comparison of different monitoring systems

To assess the relative performance of the four FC systems, we grouped the measurements into four intervals corresponding to periods of increasing or decreasing trends in CH_4 flux and shown as shaded areas in Fig. 5. It is clear from the flux data that all four systems measured the same trends in fluxes despite the apparent difference in values during some concurrent measurements. When considering just the data in each interval, we find that all systems measured similar ranges and mean values (Fig. 11). Considering just each team's mean flux for an interval and computing the standard deviation of the four mean values, we find that the standard error of a team's mean value ranges from 4% to 20% (Table 3).

Table 3. Mean and standard deviation of the mean CH_4 flux (mg-CH_4 m^{-2} d^{-1}) measured by all teams during the four periods shown in Figure 7.

	22 June 2012			23 June 2012
Team	12:50–13:50	13:50–14:30	14:30–16:10	13:20–16:00
SINTEF	3.53	2.33	2.93	1.58
HQEI	2.68	2.49	2.83	1.45
CAS	2.73	2.70	3.13	
CSIRO	4.03	3.57	3.03	1.80
Average Flux	3.24	2.77	2.98	1.61
S.d.	0.654	0.553	0.129	0.177
Std error	0.202	0.199	0.043	0.110

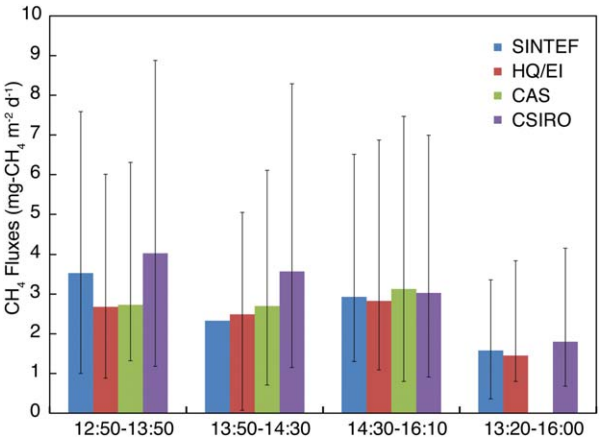

Fig. 11. Mean CH_4 flux (colored columns) and range (bars) measured by each team during the four periods identified in Figure 7.

Performance of the SINTEF triplicate system

SINTEF flux results were the averages of values determined independently for each of the three chambers connected to the gas analyzer. On some occasions, fewer chambers were used if the data quality for a chamber was assessed as unacceptable. Table 4 shows that both CO_2 and CH_4 fluxes obtained by the multiple SINTEF chambers were highly correlated in many instances, that is, there were no significant

Table 4. Interchamber comparison of CO_2 and CH_4 fluxes measured by SINTEF's triplicate system. Slope denotes the ratio of fluxes measured between pairs of chambers 1 (CH1), 2 (CH2), and 3 (CH3).

	CH_4 fluxes		CO_2 fluxes	
	Slope	R^2	Slope	R^2
	Data on 0622			
CH1 vs. CH2	1.085	0.904	0.758	0.762
CH1 vs. CH3	0.847	0.437	1.180	0.861
CH2 vs. CH3	0.946	0.710	1.330	0.825
	Data on 0623			
CH1 vs. CH2	0.701	0.904	0.709	0.807
CH1 vs. CH3	0.099	0.062	0.536	0.446
CH2 vs. CH3	−0.010	0.000	0.764	0.564
	All data			
CH1 vs. CH2	1.072	0.923	0.776	0.748
CH1 vs. CH3	0.929	0.518	1.032	0.762
CH2 vs. CH3	0.995	0.740	1.136	0.744

differences between chambers for CO_2 ($p = 1.000$) or CH_4 ($p = 0.857$) fluxes.

Despite the seemingly significant biases for individual gases on specific days, there was no systematic bias when considering all flux data for both days.

Statistics of fluxes measured by different systems

The results of one-way analysis of variance (ANOVA) indicated that there were no significant differences in CH_4 ($p = 0.889$) and CO_2 ($p = 0.176$) fluxes measured by the four teams (Table 5). The significance level (p) was relatively higher for CH_4 than CO_2 fluxes when comparing results between teams. The lower significance for CO_2 fluxes might reflect more variable CO_2 concentrations due to short-term changes in environmental conditions, for example, solar input, photosynthesis, and respiration of phytoplankton on different sides of the boat. This makes it difficult to distinguish between the impacts of system design from influences caused by changing environmental conditions. In a given water mass, the potentially more stable dissolved CH_4 concentration (not subject to significant diurnal changes due to photosynthesis and respiration) suggests that CH_4 is a more suitable tracer gas for such intercomparison experiments to determine the impacts of difference in system design.

Testing the TBL model

Correlations between the measured CO_2 and CH_4 fluxes and wind speed (Fig. 12) give an indication of how well the TBL model applies under conditions during the experiment. To accomodate the influence of changes in surface water pCH_4 on the CH_4 flux, the measured fluxes were normalized by the corresponding pCH_4 values (Fig. 12c). For 22 June,

Table 5. Results (p-value) of one-way ANOVA analysis of CH_4 and CO_2 fluxes measured by different teams.

	CH_4	CO_2
All groups	0.889	0.176
SINTEF vs. HQ/EI	0.706	0.098
SINTEF vs. CAS	0.998	
SINTEF vs. CSIRO	0.723	0.115
HQ/EI vs. CAS	0.683	
HQ/EI vs. CSIRO	0.439	0.696
CAS vs. CSIRO	0.699	

the pCH_4 data were linearly interpolated in time prior to normalization of the corresponding fluxes.

Normalization of the CH_4 fluxes significantly improved the goodness of fit from an R^2 of ~ 0.5 to > 0.8. Note that these correlations are strongly influenced by the sparse number of data points for wind speeds > 2.5 m s^{-1}, which produce unrealistically high R^2 values for the linear regressions.

Considering only regressions of the normalized CH_4 fluxes against wind speeds ≤ 3 m s^{-1} yielded very low correlations for all of the teams ($0.0005 \leq R^2 \leq 0.34$, Fig. 13, Table 6), suggesting other non-wind related processes play a relatively more important role in determining the gas flux at low wind speeds. However, inspection of Fig. 5 shows very similar overall patterns in both CH_4 flux and wind speed, suggesting that the use of lagged wind speed data may provide a superior correlation, that is, peaks in flux appear to trail peaks in wind speed by 30–50 min. Note, however, that the apparent lag time also reflects the timing of the chamber deployments relative to the timing of changes in the environment.

Although several of the teams had previously encountered significant persistent spatial gradients in pCH_4 in other reservoirs, the rapid change in pCH_4 at a fixed location came as a surprise and highlights the value (and need) of high temporal resolution measurement of dissolved gas concentration.

The offset in time between observed changes in pCO2 and pCH_4 on 22 June 2012 (Figs. 7 and 8) suggests a decoupling between the processes responsible for large diurnal changes in dissolved CO_2, that is, photosynthesis and respiration, and the advection of water masses that we believe account for the change in pCH_4. We infer from these data that the spatial distribution of phytoplankton in the tributary was more uniform than distribution of dissolved CH_4.

Methodological factors

Chamber shape effect

We did not find strong evidence of an effect of chamber design on the measured fluxes. This may reflect the low wind speed conditions prevalent during most of the experiment, that is, very low surface drift velocities, no wakes, etc.,

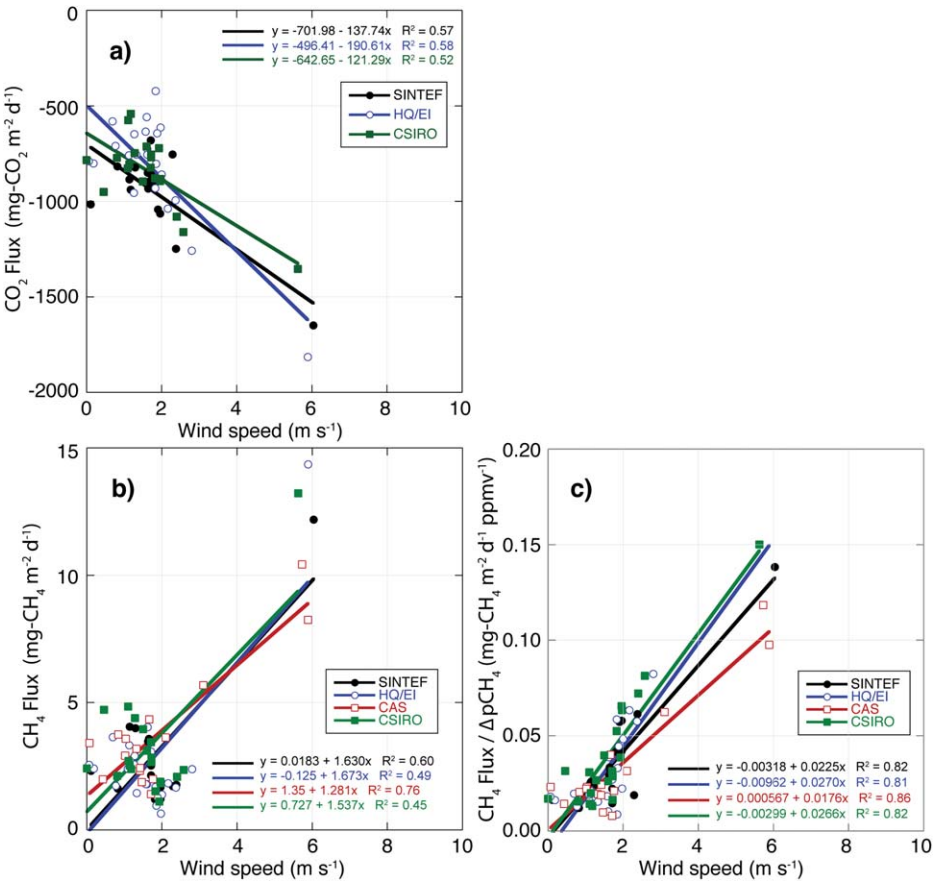

Fig. 12. Trace gas fluxes as a function of wind speed for (a) CO_2; (b) CH_4; and (c) CH_4 normalized by ΔpCH_4.

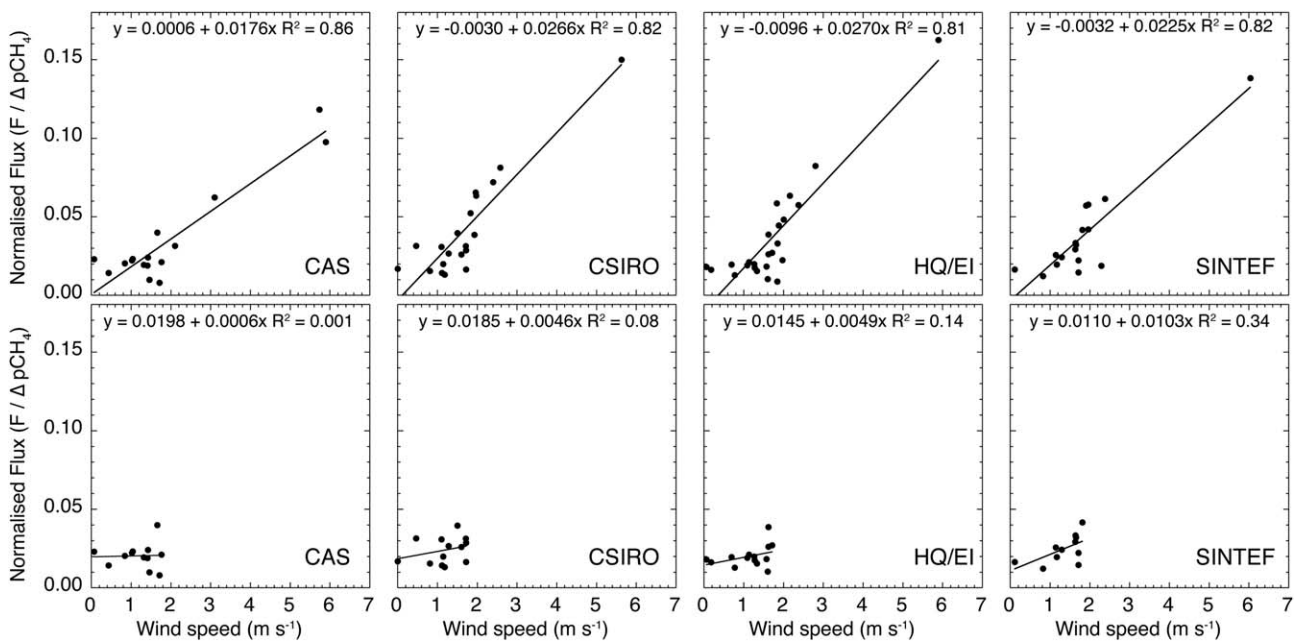

Fig. 13. Normalized CH_4 flux vs. wind speed (top) for all data and (bottom) for wind speed < 1.8 m s^{-1}.

will not generate much turbulence along the submerged edges of the chambers.

Given the prevalence of low wind conditions in many parts of the world, especially in coastal waters of SE Asia (Chen et al. 2013), we recommend that researchers NOT apply a chamber shape correction to data collected at wind speeds < 2 m s^{-1}.

Methodological uncertainty vs. natural small-scale variability

The close qualitative correspondence between wind speed and normalized flux trends in addition to the similar "interval" mean fluxes (Table 3) measured by each group suggests that short-term, small-scale variability in fluxes was responsible for most of the differences between the different teams' measurements rather than any bias associated with the different methodologies.

Variability between SINTEF triplicate measurements

The triplicate chamber system has the potential to provide additional statistical confidence to flux measurements over a given interval. It is particularly well suited to measurement of systems dominated by diffusive fluxes. However, the triplicate method requires more demanding analysis in that the data record must be partitioned into three different groups and allowance must be made for the response time of the overall system to ensure regressions for one chamber are not contaminated by legacy concentration data from other chambers. This method also runs the risk of not accurately capturing sudden changes in fluxes if there is an insufficient number of measurement "bursts" for each chamber.

The CSIRO team experimented with a similar "duplicate" measurement system in subtropical Australia in 2009 and found it unsuitable for systems with significant bubble activity because of the risk of the gas concentration in a chamber increasing beyond the range of the gas analyzer while a different chamber was being sampled. This resulted in an unacceptable number of deployments being discarded because it was impossible to determine concentration changes over a suitable time interval that included the contribution of the bubbles.

Spatial gradients in bubble activity and pCH_4

Our hypothesis of water masses with different pCH_4 being responsible for the observed change in pCH_4 on 22 June requires the presence of a spatial gradient in dissolved CH_4 which in turn requires a gradient in CH_4 production rate and/or varying water column depths that would allow different amounts of gas to dissolve from bubbles as they pass through the upper few meters of the water column. Although highly speculative, this would be consistent with the hydroacoustic observation of the most intense bubble activity occurring downstream of the measurement site on 22 June combined with the northwesterly northerly surface drift that the wind regime would have produced. Alternatively, the sediments in this tributary are likely organic rich as the result of local fish farming and agricultural activities in the catchment with the highest CH_4 production occurring in deposition zones and tapering off in the downstream direction as has been observed by several of the teams in other reservoirs (DelSontro et al. 2010; Sherman et al. 2012).

Table 6. Linear regression coefficients for CH_4 flux normalized by pCH_4 vs. wind speed using all data from 22 June 2012 to 23 June 2012 and after applying a low-pass filter for wind speeds < 1.8 m s^{-1}.

Wind speed filter		EI	CSIRO	CAS	HQ/EI
All data	Intercept	−0.00962	−0.00299	0.000567	−0.00318
All data	Slope	0.0270	0.0266	0.0176	0.0225
All data	R^2	0.807	0.824	0.864	0.821
$u<1.8$	Intercept	0.0145	0.0185	0.0198	0.0110
$u<1.8$	Slope	0.00494	0.00462	0.000561	0.0103
$u<1.8$	R^2	0.143	0.0813	0.00131	0.344

Comments and Recommendations

Through this intercomparison experiment, participants from CAS, CSIRO, SINTEF, and HQ\EI measured very similar fluxes using independent measuring systems. The results indicate that the FC measurement method appears to be accurate to better than ± 20% in a reservoir with little or no obvious ebullition. The differences between concurrent measurements reflect small-scale variability in the underlying factors (e.g., pCH_4, water turbulence) that govern gas transfer processes. The shape and dimensions of the chambers had no discernable impact on the measured fluxes and there is no need for chamber-specific adjustments to be applied, especially when the measurements were taken under calm situations where wind speed is lower than 2 m s^{-1}.

The new generation of gas analyzers equipped with high-resolution CRDS technology can effectively capture very small changes in gas concentration allowing rapid, accurate and repeatable measurements of even small diffusive fluxes of CH_4. Their high sampling frequency allows detection and quantification of small CH_4 bubble emission events at the reservoir surface. Based on these results, we recommend that diffusive greenhouse gas fluxes from reservoirs can be directly measured using FCs connected to high precision and high sampling frequency gas analyzers.

Longer deployment durations are recommended when there are obvious changes in environmental conditions, especially wind speed, to ensure the flux characteristics before and after the change are fully captured. Recirculating systems are best suited for longer deployments as they ensure constant pressure conditions in the chamber

regardless of duration. Chambers without a recirculation system can be used only for short duration deployments.

It is important to consider wind conditions (speed, direction) and surrounding terrain characteristics when choosing sampling sites to ensure the sites are representative of the reservoir more generally. These influence the turbulence in both the water and the atmosphere. Hydroacoustic surveys facilitate site selection by identifying zones of locally higher gas production and providing valuable contextual information for the analysis of the flux measurements. Under the right conditions, the hydroacoustic method also provides additional independent quantification of bubble fluxes as they rise through the water column.

Finally, but most important for conducting intercomparison experiments with participants from around the world, it is better to have all the data checked and analyzed with all the participants gathered together shortly after the experiment. Otherwise, it risks becoming a lengthy and challenging task for a variety of reasons.

References

Barros, N., and others. 2011. Carbon emission from hydroelectric reservoirs linked to reservoir age and latitude. Nat. Geosci. **4**: 593–596. doi:10.1038/ngeo1211

Chen, C., T. Huang, Y. Chen, Y. Bai, X. He, and Y. Kang. 2013. Air-sea exchanges of CO_2 in the world's coatal seas. Biogeosciences, **10**: 6509–6544. doi:10.5194/bg-10-6509-2013

Cole, J. J., D. L. Bade, D. Bastviken, M. Pace, and M. V. de Bogert. 2010. Multiple approaches to estimating air-water gas exchange in small lakes. Limnol. Oceangr.: Methods. **8**: 285–293. doi:10.4319/lom.2010.8.285

Cole, J. J., and N. F. Caraco. 1998. Atmospheric exchange of carbon dioxide in a low-wind oligotrophic lake measured by the addition of SF6. Limnol. Oceanogr. **43**: 647–656. doi:10.4319/lo.1998.43.4.0647

Danckwerts, P. V. 1951. Sigificance of liguid-film coefficients in gas absorption. Ind. Eng. Chem. **43**: 1460–1467. doi:10.1021/ie50498a055

Deacon, E. L. 1977. Gas transfer to and across an air-water interface. Tellus. **29**: 363–374. doi:10.1111/j.2153-3490.1977.tb00746.x

Delsontro, T., D. F. McGinnis, S. Sobek, I. Ostrovsky, and B. Wehrli. 2010. Extreme methane emissions from a Swiss hydropower reservoir: Contribution from bubbling sediments. Environ. Sci. Technol. **44**: 2419–2425. doi:10.1021/es9031369

Diem, T., S. Koch, S. Schwarzenbach, and C. J. Schubert. 2012. Greenhoue gas emissions (CO_2, CH_4, and N_2O) from serverl perialpine and alpine hydropower reservoirs by diffusion and loss in turbines. Aqut. Sci. **74**: 619–635. doi:10.1007/s00027-012-0256-5

Dobbins, W. E. 1964. BOD and oxygen relationships in streams. ASCE J. Sanitary Eng. Div., **90**: 53–78.

Downing, A. L., and G. A. Truesdale. 1955. Some factors affecting the rate of solution of oxygen in water. J. Appl. Chem. **5**: 570–581. doi:10.1002/jctb.5010051008

Duchemin, E., M. Lucotte, R. Canuel, and A. Chamberland. 1995. Production of the greenhouse gases CH_4 and CO_2 by hydroelectric reservoirs of the boreal region. Global Biogeochem. Cycles. **9**: 529–540. doi:10.1029/95GB02202

Fearnside, P. M. 2002. Greenhouse gas emissions from a hydroelectric reservoir (Brazil's Tucuruí Dam) and the energy policy implications. Water Air Soil Pollut. **133**: 69–96. doi:10.1023/A:1012971715668

Gålfalk, M., D. Bastviken, S. Fredriksson, and L. Arneborg. 2013. Determination of the piston velocity for water-air interfaces using flux chambers, acoustic Doppler velocimetry, and IR imaging of the water surface. J. Geophys. Res.: Biogeosci. **118**: 770–782. doi:10.1002/jgrg.20064

Jähne, B., K. O. Münnich, and V. Siegenthaler. 1979. Measurements of gas exchange and momentum transfer in a circular wind-water tunnel. Tellus. **31**: 321–329. doi:10.1111/j.2153-3490.1979.tb00911.x

Kanwisher, J. 1963. On the exchange of gases between the atmosphere and the sea. Deep-Sea Res. **10**: 195–207. doi:10.1016/0011-7471(63)90356-5

Kelly, C. A., and others. 1997. Increases in fluxes of greenhouse gases and methyl mercury following flooding of an experimental reservoir. Environ. Sci. Technol. **31**: 1334–1344. doi:10.1021/es9604931

Liss, P. S., and P. G. Slater. 1974. Flux of gases across air-seainterface. Nature, **247**: 181–184. doi:10.1038/247181a0

MacIntyre, S., A. Jonsson, M. Jansson, J. Aberg, D. E. Turney, and S. D. Miller. 2010. Buoyancy flux, turbulence, and the gas transfer coefficient in a stratified lake. Geophys. Res. Lett. **37**: L24604. doi:10.1029/2010GL044164

Merlivat, L., and L. Memery. 1983. Gas exchange across an air-water interface: Experimental results and modeling of bubble contribution to transfer. J. Geophys. Res. **88**: 707–724. doi:10.1029/JC088iC01p00707

Münsterer, T., and B. Jähne. 1998. LIF measurements of concentration profiles in the aqueous mass boundary layer. Exp. Fluids. **25**: 190–196. doi:10.1007/s003480050223

O'Connor, D. J. 1983. Wind effects on gas-liquid transfer coefficients. ASCE J. Environ. Eng. **109**: 731–752. doi:10.1061/(ASCE)0733-9372(1983)109:3(731)

Peltola, O., I. Mammarella, S. Haapanala, G. Burba, and T. Vesala. 2013. Field intercomparison of four methane gas analyzers suitable for eddy covariance flux measurements. Biogeosciences **10**: 3749–3765. doi:10.5194/bg-10-3749-2013

Peltola, O., and others. 2014. Evaluating the performance of commonly used gas analyzers for methane eddy covariance flux measurements: The InGOS inter-comparison field experiment. Biogeosci. Discuss., **11**: 797–852. doi:10.5194/bgd-11-797-2014

Peng, T.-H., W. S. Broecker, G. G. Mathieu, and Y.-H. Li. 1979. Radon evasion rates in the Atlantic and Pacific Oceans as determined during the Geosecs program. J. Geophys. Res. **84**: 2471–2486. doi:10.1029/JC084iC05p02471

Podgrajsek, E., E. Sahlée, D. Bastviken, J. Holst, A. Lindroth, L. Tranvik, and A. Rutgersson. 2013. Comparison of floating chamber and eddy covariance measurements of lake greenhouse gas fluxes. Biogeosci. Discuss. **10**: 18309–18335. doi:10.5194/bgd-10-18309-2013

Rudd, J. W. M., R. Harris, C. A. Kelly, and R. E. Hecky. 1993. Are hydroelectric reservoirs significant sources of greenhouse gases. Ambio. **22**: 246–248. doi:10.2307/4314078

Schladow, S. G., M. Lee, B. E. Hurzeler, and P. B. Kelly. 2002. Oxygen transfer across the air-water interface by natural convection in lakes. Limnol. Oceanogr. **47**: 1394–1404. doi:10.4319/lo.2002.47.5.1394

Sherman, B., P. Ford, D. Hunt, and C. Drury. 2012. Reservoir Methane Monitoring and Mitigation–Little Nerang and Hinze Dam Case Study. Urban Water Security Research Alliance. 30 Dec 2014. Available from http://www.urbanwateralliance.org.au/publications/UWSRA-tr96.pdf

St Louis, V. L., C. A. Kelly, E. Duchemin, J. W. M. Rudd, and D. M. Rosenberg. 2000. Reservoir surfaces as sources of greenhouse gases to the atmosphere: A global estimate. Bioscience. **50**: 766–775. doi:10.1641/0006-3568(2000)050[0766:RSASOG]2.0.C.

Teodoru, C. R., Y. T. Prairie, and P. A. del Giorgio. 2011. Spatial heterogeneity of surface CO_2 fluxes in a newly created Eastmain-1 reservoir in Northern Quebec, Canada. Ecosystems. **14**: 28–46. doi:10.1007/s10021-010-9393-7

Tremblay, A., L. Varfalvy, G. Roehm, and M. Garneau. 2005. Greenhouse gas emissions—fluxes and processes: Hydroelectric reservoirs and natural environments. Springer.

Yang, L., and others. 2012. Surface methane emissions from different land use types during various water levels in three major drawdown areas of the Three Gorges Reservoir. J. Geophys. Res. **117**: D10109. doi:10.1029/2011JD017362

Yu, Z. Z., and L. L. Wang. 2011. Factors influencing thermal structure in a tributary bay of Three Gorges Reservoir. J. Hydrodyn. **23**: 407–415. doi:10.1016/S1001-6058(10)60130-8

Vachon, D., Y. T. Prairie, and J. J. Cole. 2010. The relationship between near-surface turbulence and gas transfer velocity in freshwater systems and its implications for floating chamber measurements of gas exchange. Limnol. Oceanogr. **55**: 1723–1732. doi:10.4319/lo.2010.55.4.1723

Wanninkhof, R. 1992. Relationship between wind speed and gas exchange over the ocean. J. Geophys. Res.: Oceans. **97**: 7373–7382. doi:10.1029/92JC00188

Zhao, Y., B. F. Wu, and Y. Zeng. 2013. Spatial and temporal patterns of greenhouse gas emissions from Three Gorges Reservoir of China. Biogeosciences. **10**: 1219–1230. doi:10.5194/bg-10-1219-2013

Acknowledgments

This research was supported by the Major State Basic Research Development Program of China (2010CB955904). We appreciate the support provided by Yu Liu, Yujin Zhao, and Tao Li from the Institute of Remote Sensing and Digital Earth, CAS, Xigong Yuan from the Institute of Hydrobiology, CAS, Jiaofeng Fu from the Institute of Geodesy and Geophysics, CAS, Xuguang Yang and Bo Qiu from the Water Environment Monitoring Centre of Yangtze River, and Biao Zhang and Hui Xie from the Three Gorges University through their participation in the field campaign. We also thank Li Fu, Bosi Shan, and other colleagues for logistic arrangements.

Submitted 20 July 2014
Revised 11 November 2014
Accepted 1 December 2014

Associate editor: Dr. Clare Reimers